

Thermal Magnetization Reversal in Arrays of Nanoparticles

Gregory Brown

*School of Computational Science and Information Technology, Center for Materials Research and Technology, and
Department of Physics, Florida State University, Tallahassee, Florida 32306-4120*

M. A. Novotny

School of Computational Science and Information Technology, Florida State University, Tallahassee, Florida 32306-4120

Per Arne Rikvold

*Center for Materials Research and Technology, School of Computational Science and Information Technology, and
Department of Physics, Florida State University, Tallahassee, Florida 32306-4350*

(November 4, 2018)

The results of large-scale simulations investigating the dynamics of magnetization reversal in arrays of single-domain nanomagnets after a rapid reversal of the applied field at nonzero temperature are presented. The numerical micromagnetic approach uses the Landau-Lifshitz-Gilbert equation including contributions from thermal fluctuations and long-range dipole-dipole demagnetizing effects implemented using a fast-multipole expansion. The individual model nanomagnets are $9\text{ nm} \times 9\text{ nm} \times 150\text{ nm}$ iron pillars similar to those fabricated on a surface with STM-assisted chemical vapor deposition [S. Wirth, *et al.*, J. Appl. Phys **85**, 5249 (1999)]. Nanomagnets oriented perpendicular to the surface and spaced 300 nm apart in linear arrays are considered. The applied field is always oriented perpendicular to the surface. When the magnitude of the applied field is less than the coercive value, about 2000 Oe for an individual nanomagnet, magnetization reversal in the nanomagnets can only occur by thermally activated processes. Even though the interaction from the dipole moment of neighboring magnets in this geometry is only about 1 Oe , less than 1% of the coercive field, it can have a large impact on the switching dynamics. What determines the height of the free-energy barrier is the difference between the coercive and applied fields, and 1 Oe can be a significant fraction of that. The magnetic orientations of the neighbors are seen to change the behavior of the nanomagnets in the array significantly.

The ability of the magnetization to maintain one particular orientation among many is an essential part of numerous applications of magnetic materials. The coercive field is defined to be the weakest magnetic field for which the magnetization will deterministically align with the field. For applied magnetic fields weaker than the coercive field, a free-energy barrier may separate the orientation of the magnetization from that of the applied magnetic field. In these weak fields the changes in the orientation of the magnetization occur only in the unlikely event of thermal crossing of the free-energy barrier, and magnetization switching becomes a probabilistic process. In magnetic storage, thermal magnetization switching is important for understanding the reliability of recorded data in the presence of stray fields, as well as for thermally assisted reading and writing.¹

Here we present numerical results for magnetization switching in linear arrays of weakly coupled nanoscale magnetic pillars, with each pillar's long axis oriented in the z -direction, perpendicular to the substrate. The simulations start at $t = -0.25\text{ ns}$ with zero external field and the average z -component of the magnetization, M_z , oriented in the positive z -direction. The external field is then applied according to $H_z(t) = -H_0 \cos(2\pi t/1\text{ ns})$ for $-0.25\text{ ns} < t < 0\text{ ns}$, giving a final value of $-H_0$.

The single-crystal nanomagnet pillars considered here are modeled after iron nanopillars constructed using STM-assisted chemical vapor deposition.^{2,3} The numerical model consists of magnetization vectors of magnitude unity on a cubic lattice, $\mathbf{M}(\mathbf{r}_i)$, with the motion of the vectors given by the Landau-Lifshitz-Gilbert equation,^{4,5}

$$\frac{d\mathbf{M}(\mathbf{r}_i)}{dt} = \frac{\gamma_0}{1 + \alpha^2} \mathbf{M}(\mathbf{r}_i) \times [\mathbf{H}(\mathbf{r}_i) - \alpha \mathbf{M}(\mathbf{r}_i) \times \mathbf{H}(\mathbf{r}_i)] , \quad (1)$$

where γ_0 is the gyromagnetic ratio $1.76 \times 10^7\text{ Hz/Oe}$ and $\mathbf{H}(\mathbf{r}_i)$ is the local field at each site. The local fields have contributions corresponding to exchange, dipole-dipole interactions, and random thermal noise. Underdamped precession of the spins is selected by taking the damping parameter $\alpha = 0.1$; the other material parameters were chosen to match those of bulk iron, and are 3.6 nm for the exchange length, 1700 emu/cm^3 for the saturation magnetization, and zero crystalline anisotropy. Details of the numerical model will appear in Ref. [6]. Two numerical models of the nanopillars are considered: a large-scale simulation with each pillar modeled with 4949 vectors and a simpler model with each pillar modeled with only 17 vectors.

The large-scale simulations model each $9\text{ nm} \times 9\text{ nm} \times 150\text{ nm}$ pillar using a $7 \times 7 \times 101$ lattice. For these simulations, the time-consuming dipole-dipole calculations were performed using the fast-multipole method,^{6,7} and the simulations were run on a series of massively parallel computers including a CRAY T3E and two different IBM SP's. The results reported here represent 10^5 cpu-hours of computation. The pillars were separated by twice their length, or 300 nm. At this separation the interactions between neighboring iron pillars are on the order of 1 Oe.

Here we consider linear arrays of nanopillars, 4×1 arrays in which there are two classes of pillars, which we call "inside" and "outside." The switching time for each pillar is taken to be the first time the value of M_z for that pillar passes through zero, and it is measured from $t=0$. The results are presented in Fig. 1 as $P_{\text{not}}(t)$, the probability that a pillar has not switched up to time t . A total of 30 array switches, thus 60 for each class of pillar, were simulated for $H_0=1800\text{ Oe}$ and $T=20\text{ K}$, and the results are compared to 100 switches simulated for isolated pillars under the same conditions.^{6,8} The field magnitude used here is below the coercive field for isolated nanoparticles, which has been estimated to be $1995 \pm 20\text{ Oe}$ in dynamic, nonequilibrium simulations where the field is swept linearly.⁶ From these results it appears that the outside pillars switch, on average, at earlier times than either the inside pillars of the array or the isolated pillars. We note that functional forms for $P_{\text{not}}(t)$ that are neither exponentials nor the error functions associated with Gaussian statistics have been observed experimentally.^{9,10} A simple theory with an analytic form for P_{not} reasonably describes the simulation results for isolated pillars.^{6,8}

To investigate switching involving much larger free-energy barriers, and thus longer switching times, simulations were also conducted with a simplified model of the pillars, specifically with each pillar modeled by a $1 \times 1 \times 17$ arrangement of magnetization vectors.¹¹ This models a $5.2\text{ nm} \times 5.2\text{ nm} \times 88.4\text{ nm}$ iron pillar, which has approximately the same aspect ratio as the previous pillar. For an isolated pillar of this type, the coercive field is approximately 1500 Oe. The pillars in these arrays were separated by 176.8 nm, and the dipole-dipole interactions were calculated using direct summation.^{6,11} Because this approach is $O(N^2)$ the calculation, which is fast for individual pillars, is slow for even small arrays. Still, these simulations are computationally less expensive than those discussed above, and results are presented for 1269 array switches and 1986 isolated pillar switches. The results reported here required about 10^4 cpu-hours of computation on desktop workstations.

The $P_{\text{not}}(t)$ for 4×1 arrays of the simple model with $H_0 = 1000\text{ Oe}$ and $T = 20\text{ K}$ are shown in Fig. 2, along with the results for isolated pillars under the same conditions. In this case, the differences in $P_{\text{not}}(t)$ are small, but the array pillars still appear to have a small bias to switch at earlier times than isolated pillars. Under these conditions, however, the effect of the magnetic orientation of the nearest-neighbor pillars can be seen. Fig. 3 shows subsets of $P_{\text{not}}(t)$ for the switching of inside pillars in the simple model. The dotted and dashed curves are P_{not} for inside pillars where one and both nearest-neighbor pillars have already switched, respectively. Here the switching time is measured from the last time one of the nearest-neighbor pillars switched. The data is presented on a linear-log scale, and in both cases P_{not} is consistent with an exponential form. This suggests that pillars in these environments have an approximately constant, history-independent decay rate determined by the orientation of the nearest-neighbor pillars. The exponential form is consistent with our simple theory for P_{not} in nanomagnet pillars,^{6,8} because environments with switched neighbors cannot exist for times less than t_g , the growth time from nucleation of one endcap to M_z passing through zero. The solid curve is P_{not} constructed from the data for pillars with two neighbors, neither of which have switched. The t_{sw} used for this data occur at times greater than t_g , here estimated using our simple theory^{6,8} as twice the earliest observed t_{sw} . In addition t_g has been subtracted from each t_{sw} for this curve. Similar results for the outside pillars of the array are shown in the inset of Fig. 3. The trend towards slower decay with increasing number of switched neighbors is consistent with a simple picture of dipole-dipole interaction between nearest-neighbor pillars with an unswitched neighbor contributing a field parallel to the external field and a switched neighbor contributing a field antiparallel to the external field. Currently, a sufficient number of samples do not exist to reliably repeat this analysis for the larger simulations.

To summarize, we have simulated the switching dynamics in linear arrays of nanomagnet pillars after a reorientation of the external field, both for a simple model in which each pillar is represented by a one-dimensional array of magnetization vectors and for a large-scale model with each pillar represented by a three-dimensional lattice of vectors. In one-dimensional arrays of pillars that are mutually located in the other pillars' far fields and that have small free-energy barriers, the $P_{\text{not}}(t)$ of the pillars at the end of the arrays falls off faster than that of isolated pillars and the inside pillars of the array. For pillars that have large free-energy barriers, the long switching-time tails of P_{not} for pillars with different numbers of switched nearest neighbors show exponential behavior, with decay constants that decrease with increasing numbers of switched neighbors. This occurs because the presence of unswitched (switched) neighbors enhances (retards) switching.

Supported by NSF grant No. DMR-9871455, NERSC, and by FSU/CSIT, FSU/MARTECH, and FSU/ACNS.

- ¹ J. J. M. Ruigrok, R. Coehoorn, S. R. Cumpson, and H. W. Kesteren, *J. Appl. Phys.* **87**, 5398 (2000).
² S. Wirth, M. Field, D. D. Awschalom, and S. von Molnár, *Phys. Rev. B* **57**, R14028 (1998).
³ S. Wirth, M. Field, D. D. Awschalom, and S. von Molnár, *J. Appl. Phys.* **85**, 5249 (1999).
⁴ W. F. Brown, *Phys. Rev.* **130**, 1677 (1963).
⁵ A. Aharoni, *Introduction to the Theory of Ferromagnetism* (Clarendon, Oxford, 1996).
⁶ G. Brown, M. A. Novotny, and P. A. Rikvold, in preparation.
⁷ L. Greengard and V. Rokhlin, *J. Comp. Phys.* **73**, 325 (1987); **135**, 280 (1997).
⁸ G. Brown, M. A. Novotny, P. A. Rikvold, *J. Appl. Phys.* **87**, 4792 (2000).
⁹ M. Lederman, S. Schultz, and M. Ozaki, *Phys. Rev. Lett.* **73**, 1986 (1994).
¹⁰ R. H. Koch, *et al.*, *Phys. Rev. Lett.* **84**, 5419 (2000).
¹¹ E. D. Boerner and H. N. Bertram, *IEEE Trans. Magn.* **33**, 3052 (1997).
¹² G. Korniss, G. Brown, M. A. Novotny, and P. A. Rikvold, in *Computer Simulation Studies in Condensed Matter Physics XI*, edited by D. P. Landau and H.-B. Schüttler (Springer-Verlag, Berlin, 1999), p. 134.

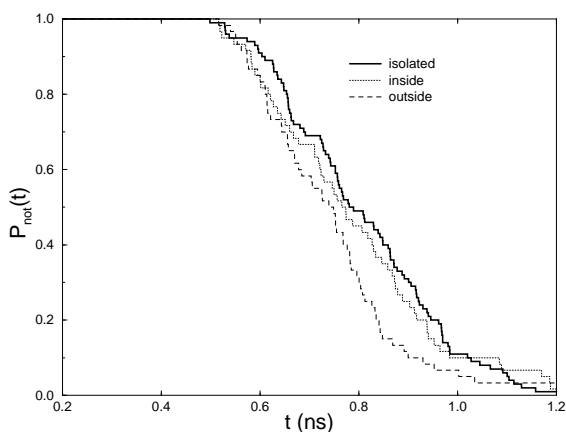


FIG. 1. Probability of not switching, P_{not} , for large-scale simulations of nanomagnet pillars in a 4×1 array. The solid curve is for isolated pillars, the dotted curve is for inside pillars, and the dashed curve is for outside pillars for 30 simulated array switches and 100 simulated isolated-pillar switches with $H_0=1800$ Oe and $T=20$ K.

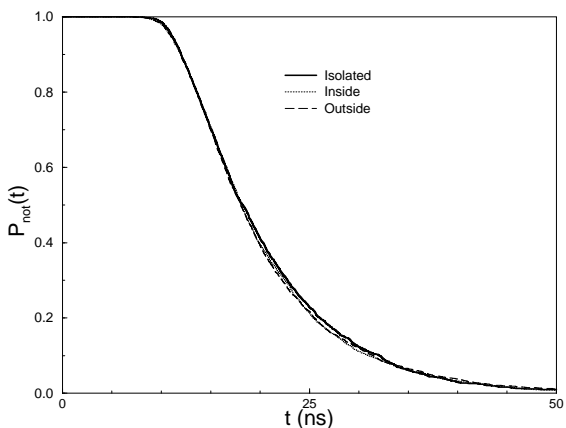


FIG. 2. Probability of not switching, P_{not} , for simulations of a simple model of nanomagnets in a 4×1 array. The solid curve is for isolated pillars, the dotted curve is for inside pillars, and the dashed curve is for outside pillars. These results are for 1269 simulated array switches and 1986 simulated isolated-pillar switches at $H_0=1000$ Oe and $T=20$ K. The free-energy barrier in this reversal is higher than for the results shown in Fig. 1.

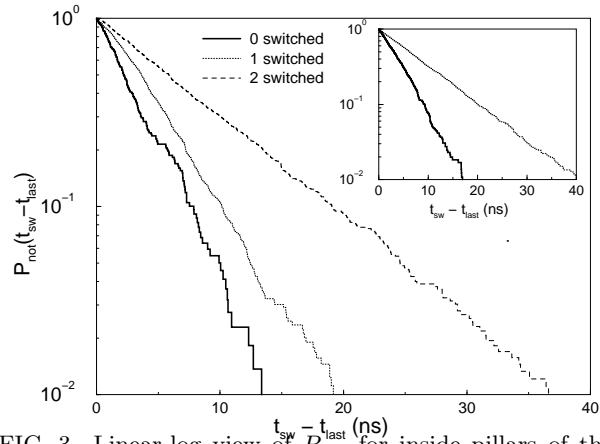


FIG. 3. Linear-log view of P_{not} for inside pillars of the simple model with different orientations of the nearest-neighbor pillars. The dotted and dashed curves are for one and both neighbors switched, respectively, and the switching time, t_{sw} , is measured since the last time a neighbor switched. The solid curve is the exponential tail of P_{not} for pillars with both neighbors unswitched, shifted along the x -axis by the growth time, t_g . Similar results are shown for the outside pillars in the inset.